ORIGINAL RESEARCH

Polyethylenimine grafted H_2O_2-oxidized cellulose membrane as a novel biosorbent for Cr(VI) adsorption and detoxification from aqueous solution

Shengli Zhang · Haoyu Chen · Silue Zhang · Chengcheng Kai ·
Man Jiang · Qun Wang · Zuowan Zhou

Abstract A novel biosorbent PEI-HOCM was successfully prepared by grafting polyethyleneimine (PEI) onto H_2O_2-oxidized cellulose membrane (HOCM). The whole systhesis process occurred in aqueous solution and was environmentally friendly without any toxic cross-linkers involved. ATR-FTIR, XPS and titration analysis confirmed that the hydroxyl groups of cellulose were oxidized to carbonyl groups by H_2O_2 and PEI was successfully introduced to the HOCM. The PEI-HOCM had positively charged surface ($+ 20.6$ to $+ 86.6$ mV) at the measured pH range 3–9 according to the zeta potential analysis. The adsorption of Cr(VI) on the PEI-HOCM obeyed the pseudo-second-order kinetic model and Langmuir isotherm model. Its maximum equilibrium adsorption capacity was 147.06 mg/g at 25 °C, which was much higher than that of cellulose membrane (CM, 30.61 mg/g). According to the obtained results from the intraparticle diffusion, Body kinetic and diffusion-chemisorption models, film diffusion was the rate-limiting step and chemical adsorption was the main mechanism of Cr(VI) adsorption. The Cr(VI) adsorbed on the PEI-HOCM was completely reduced to Cr(III), suggesting that PEI-HOCM was not only useful for Cr(VI) removal but also good for its detoxification. The competitive uptakes from coexisting components (Na^+, Mg^{2+}, Ca^{2+}, phenol, Cl^- and NO_3^-) were insignificant except $H_2PO_4^-$ and SO_4^{2-} which reduced the Cr(VI) uptake with a efficiency loss of 22–41%. Ionic strength had little effect on the adsorption in the range of 0–1000 mg/L NaCl. After five adsorption/desorption cycles, the PEI-HOCM still retained good adsorption capacity. More importantly, it can be separated easily after adsorption, which will greatly benefit the wastewater treatment by simplifying the separation procedure and reducing costs.

Keywords Polyethylenimine (PEI) · Cellulose membranes · Oxidized cellulose · Adsorption · Hexavalent chromium

S. Zhang (✉) · S. Zhang · C. Kai · Q. Wang
School of Geosciences and Environmental Engineering,
Southwest Jiaotong University,
Chengdu 610031, Sichuan, China
e-mail: zhang222@home.swjtu.edu.cn

H. Chen
LongPing Branch, Graduate School of Hunan University,
Changsha 410125, Hunan, China

M. Jiang · Z. Zhou (✉)
School of Materials Science and Engineering, Southwest
Jiaotong University, Chengdu 610031, Sichuan, China
e-mail: zwzhou@swjtu.edu.cn

Introduction

Cr(III) and Cr(VI) are the two main oxidation states of chromium in aqueous systems. Compared with Cr(III), Cr(VI) is more toxic due to its higher water solubility, stronger oxidative activity and more significant cytotoxicity (Yan et al. 2017). Cr(VI) is widely used in many industries, such as chromic salt manufacturing, electroplating, alloying, leather tanning, textile dying, wood preservation, and etc. (Chen et al. 2011; Ma et al. 2014). Therefore, the removal of Cr(VI) from wastewater is an urgent and necessary environmental issue. Numerous technologies have been developed for the treatment of Cr(VI)-rich wastewater, for instance, chemical reduction and precipitation, membrane separation, ion exchange, electrodialysis, and adsorption (Barrera-Diaz et al. 2012; Jiang et al. 2018). Among them, adsorption is the most used technology owing to its simple design, easy operation and low operation cost.

A variety of adsorbents, including activated carbon (Gupta et al. 2013; Leila et al. 2018), synthetic polymer (Kera et al. 2016), biomass (Miretzky and Cirelli 2010) and minerals (Alemayehu et al. 2011) have been adopted for treating Cr(VI)-contaminating wastewater. In particular, using renewable and biodegradable lignocellulosic materials as low-cost adsorbents has received great attention in recent years (Safari et al. 2018; Ge and Li 2018). Cellulose, as the most abundant polymer in nature, has attracted great attention due to its renewability, low cost, biocompatibility and nontoxicity (Cranston et al. 2010; Kaya et al. 2016). However, the OH groups in unmodified cellulose tend to form intermolecular and intramolecular hydrogen bonds, limiting its adsorption capacity for heavy metal ions. Selective oxidation can convert the hydroxyl groups on cellulose molecules to aldehyde and/or carboxyl groups, which can provide more active sites for the further modification of cellulose. Nowadays, the widely used oxidizing agents mainly are periodate (Kumari et al. 2016; Zhang et al. 2017b) and TEMPO (Lin et al. 2017; Zhao et al. 2017). Comparatively speaking, hydrogen peroxide (H_2O_2) is an environmentally friendly and cost-effective oxidizing agent (Zhang et al. 2017a; Sudur and Orbey 2015). Moreover, the H_2O_2-mediated oxidation is done under mild conditions, which can limit the decrease in molecular weight of cellulose.

Polyethyleneimine (PEI), a cationic polymer containing a large number of amino groups on the macromolecular chain, exhibits strong chelation property for heavy metals (Setyono and Valiyaveettil 2016; Chen et al. 2014). But due to its high solubility in water, the PEI must be immobilized on solid supports through grafting or cross-linkin before application. Currently, most researches focus on the cross-linking approach, where traditional toxic cross-linkers such as epichlorohydrin (Ge et al. 2016; Liu et al. 2011) and glutaraldehyde are involved (Yan et al. 2017; Wang et al. 2017). Recently, Zhao et al. (2017) reported a successful synthesis of polyethylenimine-cross-linked cellulose nanocrystals (PEI-CNC) in the presence of condensing agent EDC and coupling reagent NHS. Though traditional toxic cross-linkers were avoided, the oxidation of nanocrystals was done by TEMPO system. Moreover, the PEI-CNC was difficult to be separated from a solution system when it was used as an adsorbent. The reported methods employed to solve this problem commonly rely on the introduction of magnetic materials (Sun et al. 2014; Zheng et al. 2018). In our previous study, polyethylenimine functionalized Fe_3O_4/steam-exploded rice straw composite was synthesised, which had high adsorption capacity toward Cr(VI) and was easily separated from the aqueous solution by an ordinary magnet (Zhang et al. 2018). Unfortunately, a toxic cross-linker glutaraldehyde was used. Furthermore, the existence of magnetic materials might increase the processing difficulty and cost when magnetic adsorbents were discarded.

On the basis of these considerations, a novel biosorbent PEI-HOCM was prepared by grafting polyethyleneimine (PEI) onto H_2O_2-oxidized cellulose membrane (HOCM) in this study. The whole reaction process occurred in aqueous solution and was environmentally friendly with H_2O_2 as an oxidizing agent and without toxic cross-linkers involved. Moreover, the membrane adsorbent had no separate problem compared with powder adsorbents. The as-prepared samples were carefully characterized by scanning electron microscopy (SEM), attenuated total reflectance-Fourier transform infrared spectroscopy (ATR-FTIR), X-ray diffraction (XRD), X-ray photoelectron spectroscopy (XPS), zeta potential and titration analysis. Its adsorption property for Cr(VI) was investigated in batch experiments. In addition, the effects of ionic strength and co-existing components

(Na^+, Mg^{2+}, Ca^{2+}, phenol, Cl^-, NO_3^-, $H_2PO_4^-$ and SO_4^{2-}) and the reusability of PEI-HOCM were evaluated.

Experiments

Materials

Cotton pulp cellulose was provided by Bailu Chemical Fiber Group Ltd. (Xinxiang, China), with DP of 550 and 95% α-cellulose. The pulp has been smashed and dried in a vacuum oven (60 °C) for 5 h before dissolution. Tetrabutylammonium hydroxide (TBAH, 15 wt%) solution was provided by Runjing Chemical Co. Ltd. (Zhenjiang, P. R. China), which was concentrated through distillation under reduced pressure (− 98 kPa, 50 °C). The TBAH working solution of desired concentration was prepared by diluting its stock solution with deionized water after calculating the content of TBAH by acidimetry. Dimethylsulfoxide (DMSO) was supplied by Chengdu Kelong Chemical Reagent Co. (Chengdu, China).

Branched polyethylenimine (PEI, molecular weight 10,000, 99%) was purchased from Shanghai Aladdin Bio-Chem Technology Co., Ltd. Potassium dichromate ($K_2Cr_2O_7$) and hydrogen peroxide (H_2O_2, 30%) were obtained from Chengdu Jishan Chemical Co., Ltd. Other reagents were analytical grade and used without any further purification.

Preparation of cellulose membrane (CM)

Cellulose membrane (CM) was prepared following the method described in Cao's paper (Cao et al. 2018). Briefly, cotton pulp (2.5 g) was swelled in DMSO (37.5 g) for 15 min at room temperature. The cellulose was then dissolved by adding TBAH solution (10 g, 50 wt%) and stirring for 1 h at room temperature. The air bubbles in the solution were defoamed in vacuum, and the transparent cellulose solution was cast on a glass plate to give a gel membrane with ca. 0.5 mm thickness. After that, the solution was aged for 3 h at ambient atmosphere. The resulting gel membrane was subsequently washed with distilled water to remove the solvent, and the obtained CM was kepted in distilled water until use.

Preparation of H_2O_2-Oxidized cellulose membrane (HOCM)

H_2O_2-Oxized cellulose membrane (HOCM) was prepared using the following procedure: 1 g of CM was immersed in 50 mL of H_2O_2 solution with different initial concentrations (0–0.8 wt%). The mixture was placed into a magnetic stirring water bath pot and stirred for different time (30–180 min) at given temperature (25–95 °C). The desired pH (1.0–9.0) was adjusted using 1 mol/L NaOH and 1 mol/L HCl. Thereafter, the oxidized cellulose membranes was washed with distilled water and denoted as HOCM.

Synthesis of PEI grafted H_2O_2-oxidized cellulose membrane (PEI-HOCM)

1 g of HOCM was immersed in 50 mL of PEI solution with different initial concentrations (0–6 wt%). The mixture was stirred for different time (5–120 min) at room temperature. The desired pH (3.0–13) was adjusted using 1 mol/L NaOH and 1 mol/L HCl. Subsequently, the aminated cellulose membrane was washed with distilled water and oven-dried at 105 °C to finally obtain the adsorbent PEI-HOCM.

CM and HOCM were also oven-dried at 105 °C to prepare blank and reference samples.

Characterization and analysis

The physical morphologies of the CM, HOCM and PEI-HOCM were observed via a JSM-7001F (JEOL Com., Japan) electron microscope. The samples were coated with a gold film to improve their conductivity and the quality of SEM images. The surface functional groups of the CM, HOCM, PEI-HOCM and Cr-loaded PEI-HOCM were examined using a FTIR spectroscope (Nicolet 6700, Thermo Fisher Scientific, America). The data in the range of 4000–400 cm^{-1} were recorded with an ATR accessory at a spectral resolution of 4 cm^{-1}. The crystal structures of the samples were determined by X-ray powder diffraction (XRD, PANalytical X'Pert PRO, Holland). The scan was collected in the 2θ range from 5° to 60° using Cu Kα radiation (λ = 0.15418 nm) operated at 40 kV and 25 mA. The surface chemical compositions of the CM, HOCM, PEI-HOCM and Cr-loaded PEI-HOCM were analyzed by XPS on an XSAM800 electron spectrometer (Kratos, UK) with an Al Kα source. The

Cr $2p$ peaks were deconvoluted into the components consisting of a Gaussian/Lorentzian line shape function.

The surface charge property of the PEI-HOCM was measured using a SurPass3 Electrokinetic Analyzer (Anton Paar, Austria) under different pH conditions. A 0.001 mol/L of KCl solution served as the electrolyte for the measurement.

The content of the aldehyde, carboxyl and amino groups of the HOCM, PEI-HOCM and Cr-loaded PEI-HOCM was determined by titration methods. The detailed procedures were described in the supplementary material.

Batch adsorption experiments

A stock solution (1000 mg/L) of Cr(VI) was prepared from $K_2Cr_2O_7$. Working solutions of the desired concentrations were obtained by further dilution. The batch adsorption experiments were undertaken in a series of Erlenmeyer flasks (100 mL). A amount of 0.02 g of PEI-HOCM was placed into 25 mL Cr(VI) solution with different initial concentrations (25–150 mg/L). The mixture was shaken in an orbital shaker at 150 rpm for designated time (5 min–24 h) at given temperature (5–45 °C). The initial pH was adjusted to the set value (1.0–9.0) using 1 mol/L NaOH and 1 mol/L HCl. After each adsorption test, the residual Cr(VI) in the solution was measured by atomic adsorption spectrophotometer (Hitachi Z-5000, Japan). The adsorption capacity (q mg/g) was calculated according to Eq. (1).

$$q = \frac{(C_0 - C_t) \times V}{m} \tag{1}$$

where C_0 and C_t (mg/L) are the concentrations of Cr(VI) in solution before and after treatment, m (g) is the adsorbent mass, and V (L) is the volume of Cr(VI) solution.

The effects of ionic strength and co-existing components on Cr(VI) adsorption were investigated in the presence of various concentrations of different electrolyte solutions. The concentration of Cr(VI) was kept at 100 mg/ L. The ionic strength concentrations in the form of NaCl varied from 25 mg/L to 10 g/L. The co-existing components included Na^+, Mg^{2+}, Ca^{2+}, phenol, Cl^-, NO_3^-, $H_2PO_4^-$ and SO_4^{2-}, each of which was maintained at the concentrations of 300 and 600 mg/L, respectively.

The reusability of PEI-HOCM was evaluated by testing its adsorption capacity for Cr(VI) over five cycles. When the adsorption equilibrium was reached in 100 mg/L of Cr(VI) solution, the Cr-loaded PEI-HOCM was collected. Afterward, it was eluted for 6 h using a solution of 0.5 mol/L NaOH at 25 °C, washed repeatedly with distilled water and reused in next adsorption/desorption cycle.

Results and discussion

Preparation of the PEI-HOCM

Optimization of H_2O_2-oxidation conditions

Zhang et al. (2009) reported that the hydroxyl groups in gelatinized starch were mainly oxidized to aldehyde groups at low H_2O_2:starch molar ratios, while at high degrees of oxidation, the aldehyde groups were progressively converted into carboxyl groups. Cellulose has the similar chemical structures with starch. Hence, low concentrations of H_2O_2 were used in this study. The H_2O_2-oxidation conditions were optimized by changing the solution pH, H_2O_2 concentration, oxidation time and temperature as shown in Fig. 1. From Fig. 1a, it can be seen that solution pH and H_2O_2 concentration had a large effect on Cr(VI) adsorption. As the pH rose from 1.0 to 9.0, the adsorption capacity of PEI-HOCM for Cr(VI) firstly increased and then decreased. It was due to the fact that H_2O_2 had stronger oxidability in acidic condition. But H_2O_2 was stable when solution pH was less than 3. Hence, the optimal pH was found to be 4.0. With increasing H_2O_2 concentration from 0 to 0.4%, the Cr(VI) uptake increased rapidly from 24.57 to 99.25 mg/g. Afterwards, adsorption capacity decreased with further increasing H_2O_2 concentration. This was related to the unsynchronized reaction rate that high H_2O_2 concentration decomposed more rapidly than cellulose oxidation. Finally, 0.4% was chosen as the appropriate H_2O_2 concentration.

Figure 1b displays the effect of oxidation time and temperature on Cr(VI) uptake. A significant increase from 51.48 to 99.34 mg/g in adsorption capacity appeared with reaction time ranging from 30 to 120 min, then leveled out. This result indicated that 120 min was the proper oxidation time. At the beginning, the oxidant concentration was higher and
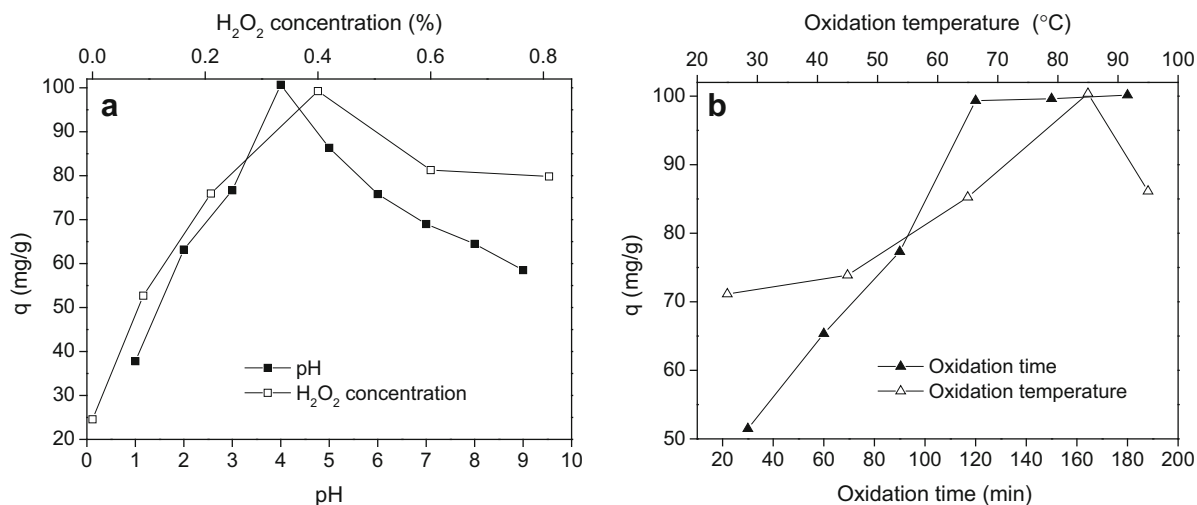
Fig. 1 Effects of solution pH, H$_2$O$_2$ concentration, oxidation time and temperature on Cr(VI) uptake by the PEI-HOCM at oxidation stage

the cellulose oxidation was easier. As the reaction was conducted, the oxidant was gradually consumed. When oxidation temperature rose from 25 to 85 °C, adsorption capacity increased from 71.13 to 100.38 mg/g. Then further increasing oxidation temperature to 95 °C, adsorption capacity dropped to 86.13 mg/g. It was the combined result that an increase of temperature resulted in the enhanced activity and the invalid decomposition of H$_2$O$_2$. Therefore, 85 °C was the optimal oxidation temperature.

Optimization of PEI-grafting conditions

The PEI grafting conditions were optimized by changing solution pH, PEI concentration and reaction time as presented in Fig. 2. From Fig. 2a, it was obvious that the adsorption capacity of PEI-HOCM for Cr(VI) increased from 62.32 to 99.09% as increasing solution pH from 3.0 to 11.0 and then decreased with the further rise of pH. The optimal pH was 11.0, which suggested that alkaline condition was beneficial to the Schiff base reaction between PEI and HOCM. But self-condensation of aldehyde groups could happen at high basicity, resulting in dropping the grafting degree of PEI. When PEI concentration increased from 0 to 3%, the adsorption capacity increased from 23.34 to 102.16 mg/g and thereafter remained almost constant. The reason was that for the fixed HOCM, the total

available aldehyde groups were limited. Therefore, 3.0% was chosen as the appropriate content.

Figure 2b shows the effect of grafting time on Cr(VI) uptake. With an increase in grafting time from 5 to 60 min, the adsorption capacity increased gradually from 62.31 to 101.24 mg/g and then reached a plateau. This result was anticipated because increasing grafting time, the reactive aldehyde groups were consumed continuously till depleted. Thus the grafting time was fixed at 60 min.

Characterization of PEI-HOCM

ATR-FTIR analysis

Figure 3 shows the ATR-FTIR spectra of the CM, HOCM and PEI-HOCM. In the CM spectrum (Fig. 3a), the strong adsorption at 3340 cm^{-1} belonged to the O–H stretching vibration. The bands in the 3000–2800 cm^{-1} range were ascribed to the C–H stretching vibration. The peak at 1642 cm^{-1} was principally contributed by the absorbed water, and the small bands in the range of 1450–1200 cm^{-1} were attributed to the C–H and O–H deformation vibrations. The prominent band at 1160 cm^{-1} was assigned to glycosidic linkages between the sugar units while the sharp peak at 895 cm^{-1} corresponded to the ring stretching of glucose. The strong adsorption between 1100 and 900 cm^{-1} was due to the C–OH deformation vibration and/or C–O stretching vibration in cellulose.
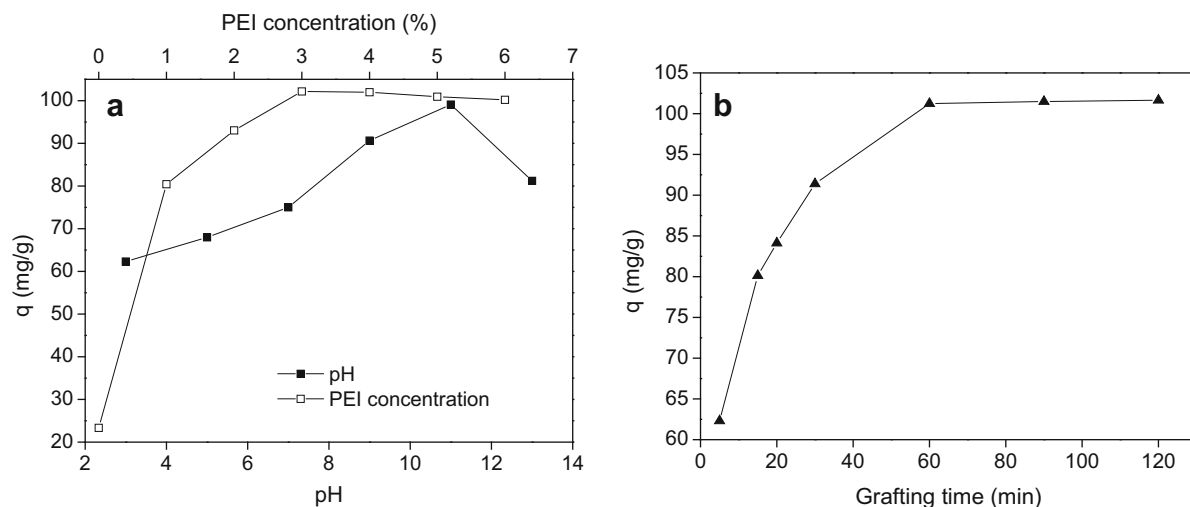
Fig. 2 Effects of solution pH, PEI concentration and graftime time on Cr(VI) uptake by the PEI-HOCM at grafting stage
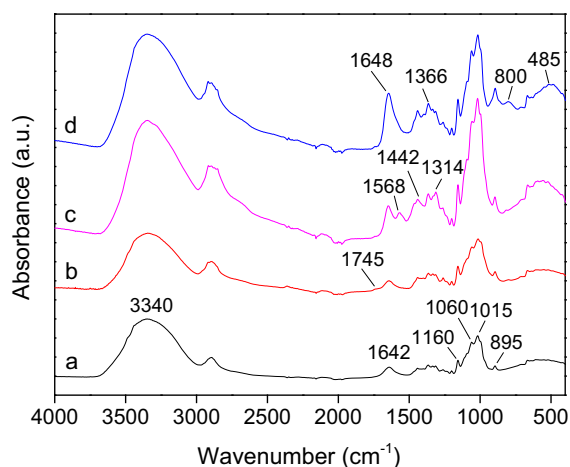
Fig. 3 FT-IR spectra of the CM (*a*), HOCM (*b*), PEI-HOCM (*c*) and Cr-loaded PEI-HOCM (*d*)

After H_2O_2 oxidation, a new adsorption appeared at 1745 cm^{-1}, which was characteristic of the C=O stretch. This feature indicated that cellulose was successfully oxidized by H_2O_2, and the hydroxyl groups on the cellulose membrane were changed to carbonyl groups.

Compared with the CM and HOCM, the ATR-FTIR spectrum of the PEI-HOCM exhibited some changes (Fig. 3c). The broad band at 3350 cm^{-1} was attributed to the overlapping of N–H and O–H stretching vibration. A new peak appearing at 1568 cm^{-1} was ascribed to the N–H bending vibration. The increased intensity at 1060 cm^{-1} was attributed to the C–N stretching. Meanwhile, the adsorption at 1745 cm^{-1} disappeared and a strong peak was observed at 1648 cm^{-1}, which revealed the C=N formation in the grafting process (Deng and Ting 2005). In additon, the C–H stretching vibration showed an obvious enhancement. The peaks at 1442 and 1314 cm^{-1} corresponding to the C–H bending vibration can be clearly observed. All these confirmed that PEI was successfully grafted to the surface of the HOCM.

Considering that several major functional groups were identified by the ATR-FTIR spectra, the content of the aldehyde, carboxyl and amino groups of the samples was determined by titration methods. The obtained results were listed in Table S1. It can be seen that the aldehyde and carboxyl content of the HOCM were 29.6 and 22.4 μmol/g after H_2O_2 oxidation, respectively, and no amine group was found. Comparatively, no aldehyde group was detected for the PEI-HOCM. The carboxyl content sharply decreased from 22.4 to 2.4 μmol/g and the amino content increased to 1.44 mmol/g. This result was in accordance with the ATR-FTIR analysis. For the Cr-loaded PEI-HOCM, the amino content varied very little. The carboxyl content was only 1.3 μmol/g, which was different from the result from ATR-FTIR. The possible reason was that the carboxyl groups formed a complex with the Cr(III).

XPS analysis

To further verify the chemical reactions taking place in the preparation process, XPS was used to analyze the surface chemical compositions of the CM, HOCM and PEI-HOCM. According to the results of XPS wide-scan spectra (Fig. 4a), the oxygen atom concentration increased from 26.67 to 35.75% after H_2O_2 oxidation and decreased from 35.75 to 29.97% after PEI grafting. The opposite change was related to the formation and consumption of aldehyde groups. Moreover, the N1s peak with binding energy at 399.8 eV can be clearly observed for the PEI-HOCM, verifying that the PEI molecules were successfully grafted onto the HOCM.

XRD analysis

The XRD patterns of the CM, HOCM and PEI-HOCM were shown in Fig. 4b. According to our previous work, the cellulose II and cellulose IV crystal structure coexisted in the CM. The diffraction peaks locating at 12.3°, 20.3° and 22.1° were respectively assigned to the $(1\bar{1}0)$, (110) and (020) planes of cellulose II (Qi et al. 2009). The diffraction peaks at 15.6° and 22.5° were for $(1\bar{1}0)$/(110) and (200) of cellulose IV crystal (Gardiner and Sarko 1985). The HOCM had almost identical XRD pattern with the CM, which demonstrated that H_2O_2 oxidation had little influence on the crystallinity. After PEI modification, the diffraction peaks of cellulose II gave a slight decrease in the

density, which was attributed to the crystalline transformation form cellulose II to cellulose IV.

SEM analysis

The SEM images of the CM, HOCM, PEI-HOCM and Cr-loaded PEI-HOCM were showed in Fig. 5. An obvious difference can be observed from the surface morphologies of the samples. Notably, the CM had a coarser surface with more cracks. After H_2O_2 oxidation, the cracks on the HOCM surface showed a decrease, revealing the reaction on the surface of the cellulose. After grafting PEI, the PEI-HOCM surface became relatively homogeneous and dense, suggesting that the introduction of macromolecular chains improved the membrane structure. For the Cr-loaded PEI-HOCM, its surface roughness further decreased because of the introduction of chromium.

Zeta potential analysis

The zeta potential of the PEI-HOCM as a function of the electrolyte solution pH was presented in Fig. S1. It can been seen that the zeta potential values firstly increased from + 46.0 to + 86.6 mV and then decreased to + 20.6 mV with the increase of the pH. The maximum value of + 86.6 mV was found at pH 3.6. Thus the PEI-HOCM had positively charged surface at the measured pH range 3–9, which can facilitate the electrostatic attraction to negatively charged Cr(VI) ions.
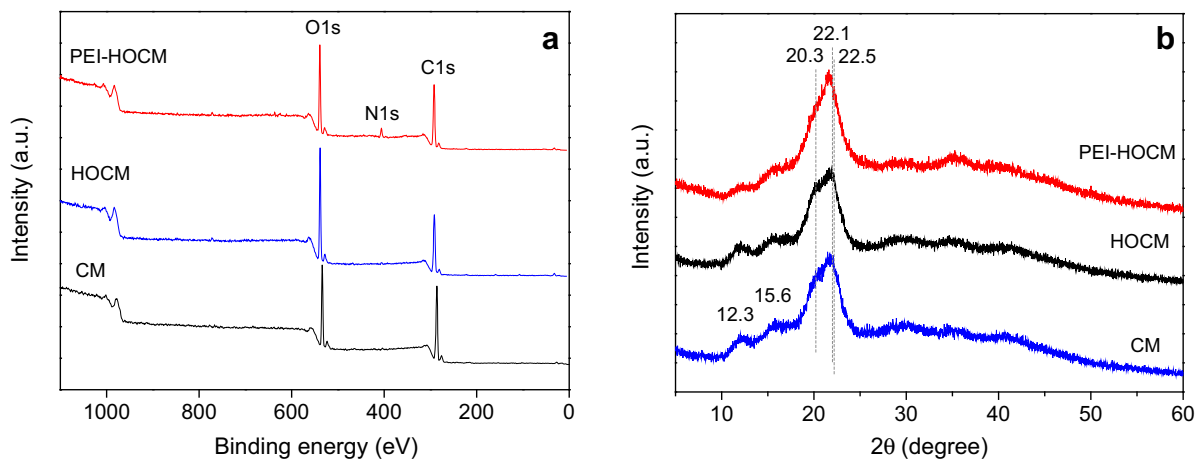
Fig. 4 XPS wide scan spectra (**a**) and XRD patterns (**b**) of the CM, HOCM and PEI-HOCM

Fig. 5 SEM images of the CM, HOCM and PEI-HOCM
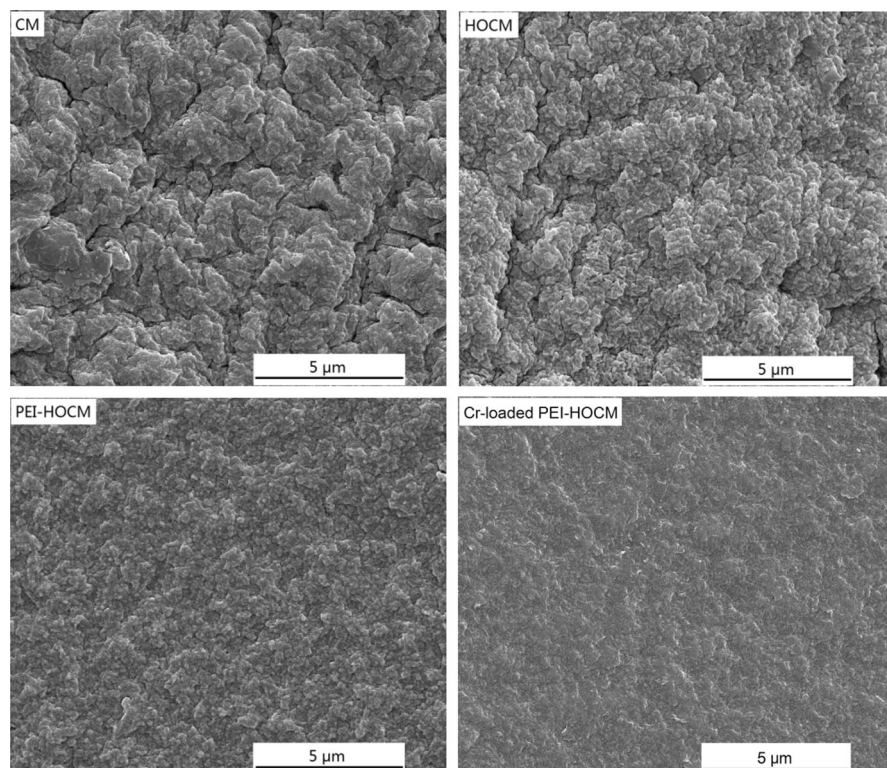
Cr(VI) adsorption on the PEI-HOCM
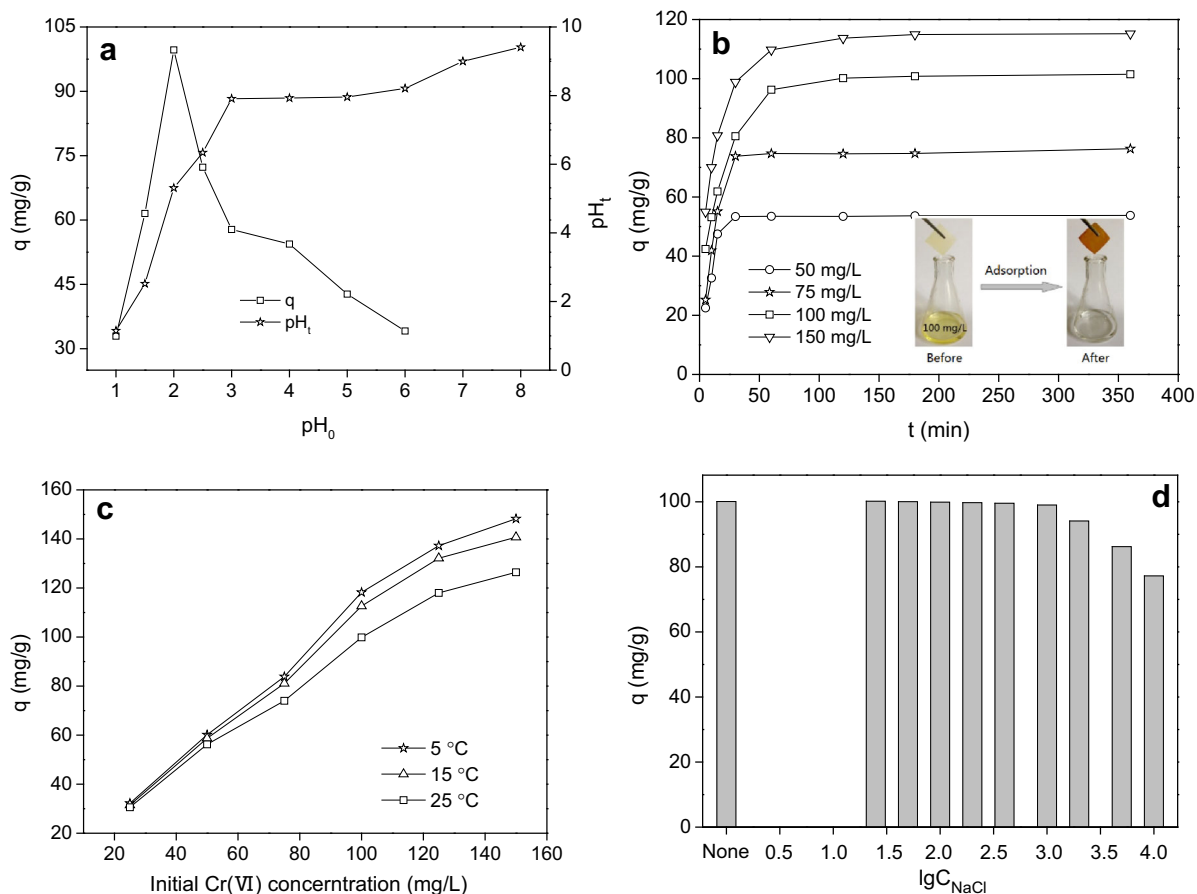
Effects of initial pH and ionic strength

The pH value of Cr(VI)-containing solution is one of the important variables in the adsorption process, affecting both the conversion of chromium species and surface properties of the adsorbent. H_2CrO_4 is the major specie at pH below 1.0, $HCrO_4^-$ is predominant in the pH range of 2.0–6.0 and CrO_4^{2-} is the main specie when pH > 6.0 (Karthikeyan et al. 2005). Hence, the effect of initial pH on Cr(VI) uptake was investigated in the pH range of 1.0–8.0 in this study as depicted in Fig. 6a. It was evident that the adsorption of Cr(VI) on PEI-HOCM was remarkably pH-dependent. The maximum uptake of Cr(VI) was found to be 2.0, which was consistent with our previous work (Zhang et al. 2018). When pH > 2.0, adsorption capacity decreased from 99.65 to 34.13 mg/g with decreasing the pH from 2.0 to 8.0, which was attributed to the deprotonation of amino groups on the PEI-HOCM and the competition of OH^-. Moreover, the adsorption free energy of CrO_4^{2-} is higher than that of $HCrO_4^-$ (Hamadia et al. 2001), with the

result that CrO_4^{2-} was less likely adsorbed than $HCrO_4^-$ at the same concentration. When pH < 2.0, Cr(VI) uptake decreased from 99.65 to 32.93 mg/g with decreasing the pH from 2.0 to 1.0. This was because Cr(VI) converted into nonionic H_2CrO_4, weakening the interation between Cr(VI) and the protonated amino groups. Therefore, the pH of 2.0 was selected as the optimal pH value for the subsequent experiments.

In addition, the final pH of the reaction system was monitored. It was interesting to note that the final pH increased rapidly from 1.15 to 7.91 when initial pH value changed from 1.0 to 3.0, and then took on a slow rise as the initial pH further increased. This might be related not only to the protonation of amino groups but also to the redox reactions between Cr(VI) and the surface groups on the PEI-HOCM.

Ionic strength is another factor affecting adsorption of a system. Figure 6d showed the adsorption capacity of the PEI-HOCM for Cr(VI) under different ionic strength. It was clear that ionic strength had little effect on the adsorption in the range of 0–1000 mg/L NaCl. With the further increase of NaCl concentration from 2 to 10 g/L, the Cr(VI) adsorption on the PEI-HOCM

Fig. 6 Effects of experimental factors on Cr(VI) adsorption by the PEI-HOCM: **a** initial pH, **b** contact time, **c** initial Cr(VI) concentration and **d** ionic strength

presented a gradual decrease. This may be attributed to the condensation of the electrical double layer and inhibition of sorbent–sorbate approaching at high ionic strength.

Adsorption kinetics

Adsorption kinetics is one of the crucial factors in the application of adsorbents. To determine the adsorption equilibrium time, the effect of contact time on Cr(VI) adsorption by PEI-HOCM was studied with initial Cr(VI) concentrations ranging from 50 to 150 mg/L at 25 °C (Fig. 6b). It is obvious that the adsorption rate of Cr(VI) by PEI-HOCM was very quick at the initial stage and then gradually decreased till the attainment of equilibrium. This can be ascribed to the availability of abundant adsorption sites on the surface of PEI-HOCM. With the active sites were increasingly

covered, it was difficult to contact the remaining adorption sites. The time required to reach adsorption equilibrium was depended on the initial Cr(VI) concentration. Upon increasing the Cr(VI) concentration from 50 to 150 mg/L, the equilibrium time increased from 30 to 180 min. From the inset of Fig. 6b, it was clear that the PEI-HOCM can be separated easily after adsorption, which will greatly benefit the wastewater treatment by simplifying the separation procedure and reducing costs.

In order to explicate the rate-controlling steps in the reaction, the adsorption kinetic data of Cr(VI) on PEI-HOCM were simulated with the pseudo-first-order and pseudo-second-order models, which were expressed as follows:

$$\lg(q_e - q_t) = \lg q_e - \frac{k_1 t}{2.303} \tag{2}$$

$$\frac{t}{q_t} = \frac{1}{k_2 q_e^2} + \frac{t}{q_e} \tag{3}$$

where q_e and q_t (both in mg/g) are adsorption capacity at equilibrium and time t, and k_1 (min^{-1}) and k_2 (g/mg min) are rate constants of pseudo-first-order and pseudo-second-order adsorption, respectively.

The linear fitting curves were shown in Fig. S2, and the related kinetic parameters were listed in Table 1. Compared with the kinetic parameters obtained from the pseudo-first-order model, the correlation coefficient (R^2) values for the pseudo-second-order kinetic model were more than 0.999 for different initial Cr(VI) concentrations. Moreover, the q_e values calculated from the model ($q_{e,cal}$) were also closer to the experimental q_e values ($q_{e,exp}$). Therefore, the pseudo-second-order kinetic equation provided a better fit to the experiment data, suggesting that the adsorption process was involved in chemisorptions through electron exchange or sharing of between adsorbents and adsorbates (Tan et al. 2016).

Adsorption isotherm analysis

Equilibrium adsorption experiments were performed by varying initial Cr(VI) concentrations from 25 to 150 mg/L at different temperatures (5, 15 and 25 °C). From the results shown in Fig. 6c, it can be observed that with the increase in the initial concentration, the Cr(VI) uptake increased. By contrast, the temperature presented a negative effect on the adsorption capacity. When the Cr(VI) concentration was above 50 mg/L, it was clear that the adsorption capacity decreased with the increase of temperature. It indicated that the adsorption of Cr(VI) on PEI-HOCM was an

exothermic reaction. This can be explained as follows: the elevated temperature enhanced the deprotonation of amino-groups and resulted in a weaker interaction between the amino groups and Cr(VI) ions (Tokuyama and Ishihara 2010).

The equilibrium data were analyzed by Langmuir and Freundlich isotherm models shown in Eqs. (4) and (5), respectively.

$$\frac{C_e}{Q_e} = \frac{1}{K_L Q_{max}} + \frac{C_e}{Q_{max}} \tag{4}$$

where K_L (L/mg) is the Langmuir equilibrium constant and is related to the adsorption energy, Q_{max} (mg/g) is the maximum monolayer adsorption capacity of the adsorbent, and C_e (mg/L) is the Cr(VI) concentration at the equilibrium.

$$\ln Q_e = \ln K_F + \frac{1}{n} \ln C_e \tag{5}$$

where K_F (mg$^{1-1/n}$ L$^{1/n}$ g^{-1}) is the Freundlich equilibrium constant related to adsorption capacity, and $1/n$ gives a measure of the intensity of adsorption. If the value of $1/n$ is lower than 1, it indicates a normal Langmuir isotherm; otherwise, it is indicative of cooperative adsorption.

The slope and intercept of each linear plot in Fig. S3 were used to calculate the Langmuir and Freundlich parameters, and the isotherm constants and correlation coefficients were summarized in Table 2. It was obvious that the adsorption of Cr(VI) on PEI-HOCM was well fitted to the Langmuir isotherm model with high R^2 (0.9991–0.9997), which may be due to the homogeneous distribution of active sites on the surface of PEI-HOCM. The Q_{max} estimated by Langmuir model was 161.29, 158.73 and 147.06 mg/g at 5, 15 and 25 °C, respectively, which was higher than that of many other adsorbents reported in the

Table 1 Kinetic parameters for the adsorption of Cr(VI) onto the PEI-HOCM

C_0 (mg/L)	$q_{e,exp}$ (mg/g)	Pseudo-first-order				Pseudo-second-order			
		$k_1 \times 10^{-3}$	$q_{e,cal}$	R^2	χ^2	$k_2 \times 10^{-3}$	$q_{e,cal}$	R^2	χ^2
50	56.21	5.27	9.31	0.2445	0.1236	5.36	54.34	0.9996	0.0024
75	75.23	1.34	70.64	0.2524	0.1683	2.15	77.52	0.9994	0.0017
100	99.21	7.12	29.17	0.5037	0.0106	1.50	101.38	0.9995	0.0005
150	115.19	6.03	34.05	0.5604	0.0729	1.55	117.65	0.9999	0.0001

Table 2 Isotherm parameters for the adsorption Cr(VI) onto the PEI-HOCM at different temperatures

T (°C)	Langmuir model				Freundlich model			
	K_L	Q_{max}	R^2	χ^2	K_F	n	R^2	χ^2
5	0.3626	161.29	0.9991	0.00002	46.37	2.601	0.9321	0.0186
15	0.2032	158.73	0.9995	0.000004	34.51	2.315	0.9447	0.0205
25	0.1259	147.06	0.9997	0.00003	26.23	2.301	0.9562	0.0277

literature (Table 3). Meanwhile, the adsorption capacity of CM was determined to be 26.23, 28.13 and 30.61 mg/g, respectively. These suggested that PEI-HOCM can be used as an efficient adsorbent for Cr(VI) removal.

Error analysis

Due to the inherent bias resulting from the linearisation of kinetics and isotherm models, the non-linear regression Chi square (χ^2) test was employed as a criterion for the fitting quality. The advantage of using χ^2 test was comparing all kinetics or isotherm models on the same abscissa and ordinate (Ho 2004). The χ^2 can be represented by Eq. (6).

$$\chi^2 = \Sigma \left[\frac{(q_e - q_{e,c})^2}{q_{e,c}} \right] \qquad (6)$$

where q_e and $q_{e,c}$ (both in mg/g) are the equilibrium capacity obtained from the experimental data and by calculation from the model, respectively. If the data from model are similar to the experimental data, χ^2 would be a small number and vice versa.

The χ^2 values of kinetics or isotherm models were shown in Tables 1 and 2, respectively. It can be seen from Table 1 that the pseudo-second-order model gave lower χ^2 values than the pseudo-first-order model. Consequently, the former was considered to be a better match for the kinetic data, which was in accordance with the result of linear regression. Compared with Freundlich isotherm model, a very low χ^2 value was obtained from Langmuir isotherm model. This result confirmed that the adsorption of Cr(VI) on PEI-HOCM obeyed Langmuir isotherm model.

Thermodynamic study

Thermodynamic parameters, Gibbs free energy change ($\Delta G°$), enthalpy change ($\Delta H°$), and entropy change ($\Delta S°$), were calculated using Eqs. (7) and (8):

$$\Delta G° = -RT \ln K_0 \qquad (7)$$

$$\ln K_0 = \frac{\Delta S°}{R} - \frac{\Delta H°}{RT} \qquad (8)$$

where R is the ideal gas constant (8.314 J/mol/K), T is the temperature in Kelvin, and K_0 (L/mol) is the adsorption equilibrium constant.

The $\Delta H°$ and $\Delta S°$ listed in Table 4 were determined from the slope and intercept of the linear plot of $\ln K_0$

Table 3 Adsorption capacity of PEI-HOCM and other cellulose-based adsorbents for Cr(VI)

Adsorbent	Q_m (mg/g)	T (°C)	References
Cell-g-GMA-β-CDN$^+$	61.05	18	Zhou et al. (2011)
Anion-exchange cellulose-based microsphere (AEM-II)	123.4	25	Zhang et al. (2012)
Glycidylmethacrylate-grafted-densified cellulose (Et-AMPGDC)	123.6	30	Anirudhan et al. (2013)
Amino-modified Fe_3O_4@SiO_2@cellulose nanocomposite (MSCGE)	171.5	25	Sun et al. (2014)
Polyethylenimine facilitated ethyl cellulose (PEI/Ecs)	36.80	25	Qiu et al. (2014)
Yeast impregnated cellulose	23.61	25	Sathvika et al. (2015)
2-Aminomethylpyridine functionalized microcrystalline cellulose microsphere (2-AMPR)	209.6	25	Dong et al. (2016)
Epichlorohydrin crosslinked carboxymethyl cellulose-ethylenediamine imprinted polymer (CL-CMC)	177.62	25	Velempini et al. (2017)
PEI-HOCM	147.06	25	This work

Table 4 Thermodynamic parameters for the adsorption of Cr(VI) onto the PEI-HOCM

$\Delta G°$ (kJ/mol)			$\Delta S°$ (J/(mol k))	$\Delta H°$ (kJ/mol)
278 K	288 K	298 K		
− 24.63	− 24.13	− 23.78	− 42.63	− 36.45

versus 1/T (Fig. S4). The negative $\Delta H°$ indicated an exothermic nature of the adsorption process, explaining the improved adsorption capacity at lower temperature. The negative $\Delta S°$ suggested the decrease of randomness at the solid/solution interface in the adsorption system. The calculated $\Delta G°$ was − 24.63, − 24.13 and − 23.78 kJ/mol at the temperatures of 5, 15 and 25 °C, respectively, which revealed spontaneous nature of the adsorption process.

Adsorption mechanisms

To further understand the adsorption mechanisms of Cr(VI) on the PEI-HOCM, intraparticle diffusion model, Body kinetics model and diffusion-chemisorption model were employed to analyze the experiment data obtained. Typically, they can be described by using Eqs. (9), (10) and (11), respectively (Cai et al. 2017; Qian et al. 2018).

$$q_t = k_{id}t^{0.5} + C \tag{9}$$

$$\frac{t^{0.5}}{q_t} = \frac{1}{q_e}t^{0.5} + \frac{1}{K_{DC}} \tag{10}$$

where k_{id} (mg/g min$^{0.5}$) is the intraparticle diffusion rate constant, C (mg/g) is a number related to the boundary layer thickness; K_{DC} (mg/g t) is the diffusion-chemisorption constant.

$$F = 1 - \left(\frac{6}{\pi^2}\right)\sum_{n=1}^{\infty}\frac{e^{-n^2}B_t}{n^2} \tag{11}$$

where B_t is a mathematical function of F. F is the fraction of adsorbate adsorbed at different time, which can be calculated by using Eq. (12):

$$F = \frac{q_t}{q_e} \tag{12}$$

For the calculated F value < 0.85, the B_t can be calculated via Eq. (13):

$$B_t = \left(\sqrt{\pi} - \sqrt{\pi - \left(\frac{\pi^2 F}{3}\right)}\right)^2 \tag{13}$$

For the calculated F value > 0.85, the B_t can be calculated via Eq. (14):

$$B_t = -0.4977 - \ln(1 - F) \tag{14}$$

Figure 7a illustrates the results of data fitting to the intraparticle diffusion model. From the plot of q_t versus $t^{0.5}$, two-stage linearity can be identified clearly. Moreover, their extending line did not pass through the origin. These findings indicated that the adsorption of Cr(VI) on the PEI-HOCM was not governed only by intraparticle diffusion and two or more steps occurred in the adsorption process (Fierro et al. 2008). The first sharper portion referred to the external mass transport between solid and liquid phase where Cr(VI) quickly diffused to the surface of the PEI-HOCM. The second stage was the intraparticle diffusion control in which the adsorbate gradually diffused into the intraparticle of the adsorbent and adsorbed onto the interior sites, finally approached to adsorption equilibrium (Sun and Yang 2003; To et al. 2017).

The Boyd model was obtained by plotting the calculated B_t versus adsorption time t as displayed Fig. 7b. It was clear that the relationship between B_t and t was neither linear nor passing through the origin, indicating that the film diffusion was the rate-controlling step of the Cr(VI) adsorption (Wang et al. 2006).

Figure 7c shows the diffusion-chemisorption model plot for the Cr(VI) adsorption on the PEI-HOCM. It was obvious that a clear inflection point can be observed from the plot. After the inflection point, the data were fitted well to the model with the R^2 values greater than 0.98. This suggested that the process can be divided to two phases (Bal Krishna et al. 2017; Qian et al. 2018): At the first few minutes, film diffusion was the dominate process, which resulted in the inflection point on the plot. After the first phase reached equilibrium, chemisorption was the
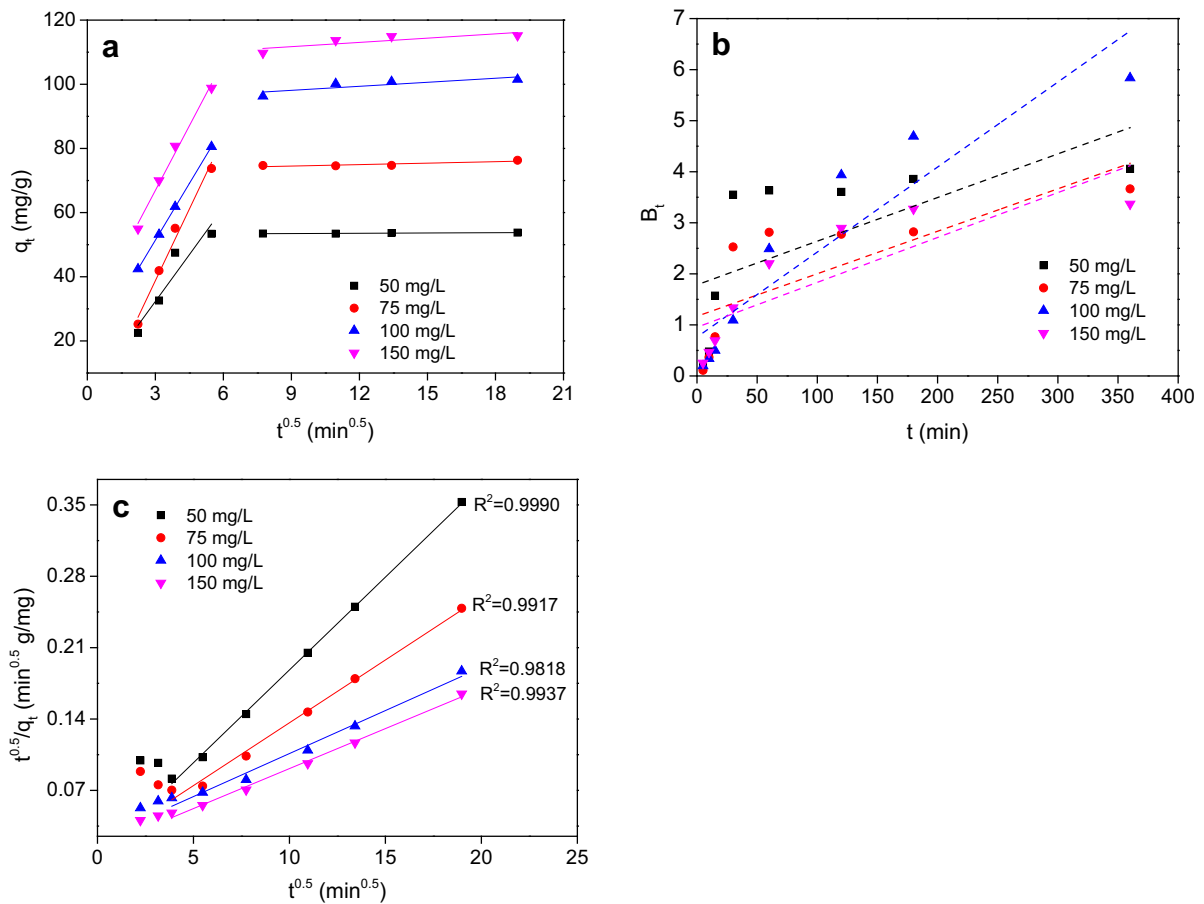
Fig. 7 Data linearly fitting using intraparticle diffusion model (**a**), Body kinetic model (**b**) and diffusion-chemisorption model (**c**)

main process, resulting in the linearity in Fig. 7c, which was further confirmed by the XPS and ATR-FTIR analysis of the Cr-loaded PEI-HOCM.

New significant bands corresponding to Cr $2p$ were evident in the XPS wide scan spectra of the PEI-HOCM treated by 50 mg/L and 100 mg/L (Fig. 8a), respectively, confirming the successful adsorption of chromium on the PEI-HOCM. The deconvolution results of the Cr $2p$ were presented in Fig. 8b. The characteristic binding energy peaks at 577.5 and 586.5 eV corresponded to Cr(III) (Stypula and Stoch 1994). No Cr(VI) was detected by Cr $2p$ XPS spectra, indicating that the Cr(VI) adsorbed on the adsorbent was completely reduced to Cr(III).

From the ATR-FTIR of Cr-loaded PEI-HOCM presented in Fig. 3d, it can be seen that the N–H bending vibration decreased obviously, suggesting that the amine groups participated in the Cr(VI) removal. The adsorption bands between 1000 and 900 cm^{-1} slightly decreased, implying that the C–OH groups also acted as active sites for the Cr(VI) removal (Wang and Lee 2011). Meanwhile, the carbonyl group (C=O) stretching vibration can be observed at 1745 cm^{-1}. The increase of the peaks at 1648 and 1366 cm^{-1} arose from the asymmetric and symmetric –COO^{-} stretching (Kumar et al. 2015). The hemiacetal groups contributed to the increases in intensity at 895 cm^{-1} (Li et al. 2011). These features clearly stated that the C–OH groups were oxidized to carbonyl groups by Cr(VI) in the adsorption process. The new peaks appearing at 800 cm^{-1} and 485 cm^{-1} were due to the formation of Cr–O bond (Ko et al. 2002; Berei et al. 2018). Hence, the resultant Cr(III) could be bound to the cellulose membrane by forming a bidentate inner-sphere complex with the carboxyl groups that resulted from the oxidation of C–OH groups by Cr(VI) (Wang and Lee 2011).
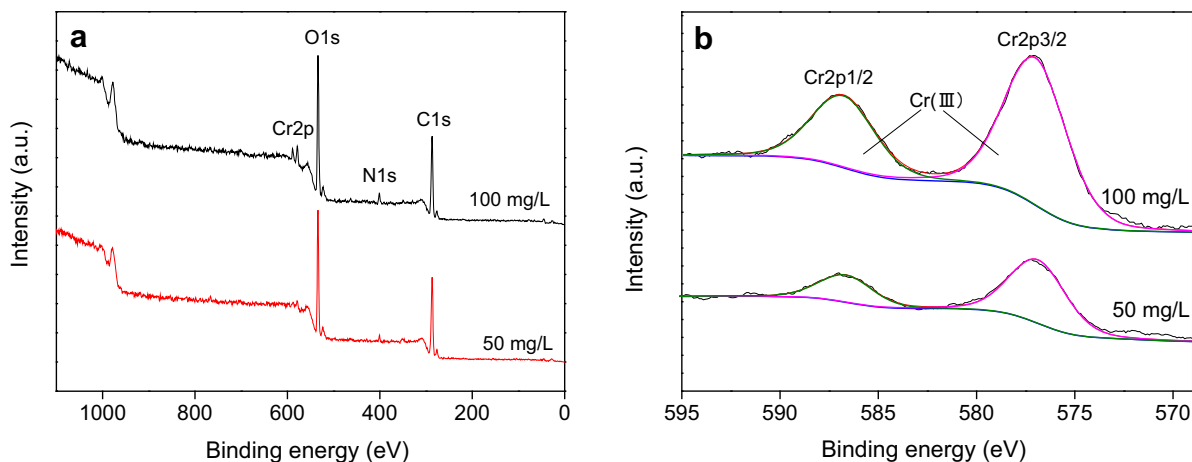
Fig. 8 XPS wide scan spectra (**a**) and Cr 2*p* spectra (**b**) of the PEI-HOCM treated by 50 and 100 mg/L Cr(VI), respectively

Effect of coexisting components and reusability of PEI-HOCM

Generally, there is more than one component in wastewater. The presence of other components may affect the adsorption efficiency of Cr(VI) to some extent. Therefore, the competitive influences of coexisting components including Na^+, Mg^{2+}, Ca^{2+}, phenol, Cl^-, NO_3^-, $H_2PO_4^-$ and SO_4^{2-} were studied as shown in Fig. 9a. It clearly indicated that Na^+, Ca^{2+}, Mg^{2+}, phenol, Cl^- and NO_3^- had very little effect on the adsorption of Cr(VI) even though their concentrations increased to six times, implying that they did not compete for the active sites on the adsorbent with Cr(VI). Meanwhile, the presence of $H_2PO_4^-$ and

SO_4^{2-} clearly reduced the Cr(VI) uptakes with a efficiency loss of 22–41%. It indicated that SO_4^{2-} and $H_2PO_4^-$ can compete for the active site to a certain extent. The negative effect of SO_4^{2-} on Cr(VI) adsorption has been reported in other literature (Zhou et al. 2016). The affinity of amino groups for SO_4^{2-} is higher than those for Cl^- and NO_3^- (Sun et al. 2013). Furthermore, aqueous SO_4^{2-} could form strong complexes with Cr(VI), which has low affinities for the surface sites (Hu et al. 2005). However, it is noteworthy that some PEI modified adsorbents can remove Cr(VI) effectively in the existence of $H_2PO_4^-$ (Sun et al. 2013). The distinct performances were mainly due to the different adsorption mechanisms. In the present study, Cr(VI) was reduced to Cr(III) in the
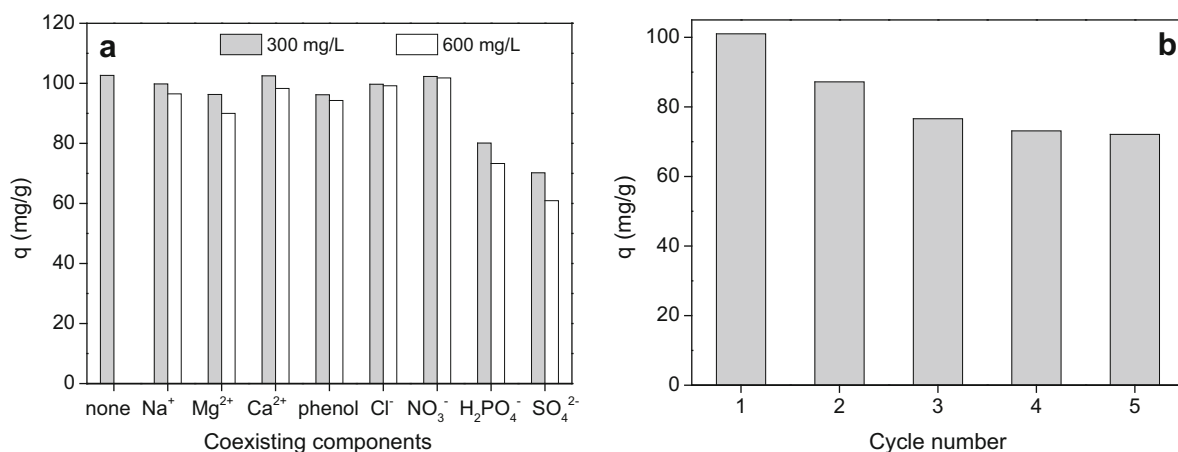
Fig. 9 Effects of coexisting components on Cr(VI) uptake by the PEI-HOCM (**a**) and regeneration performance of the PEI-HOCM over five cycles (**b**)

adsorption process. Thus the formed Cr(III) would react with $H_2PO_4^-$ to produce Cr(III)-phosphate complexes, which could cover the active sites on the surface of the PEI-HOCM and impede the access of Cr(VI).

Reusability is also one of the most critical considerations for the applicability of adsorbents. In this work, the adsorption/desorption experiments were conducted for five cycles and the results were illustrated in Fig. 9b. It was obvious that the Cr(VI) uptake capacity displayed a loss of ca. 24% after three cycles. The decrease of adsorption capacity might be because some active sites of the adsorbent reacted with Cr(VI) in an irreversible way, thus reducing the density of Cr(III) binding sites in the cycles. A similar phenomenon was observed in the case of the Cu(II) removal by TOCN-PEI (Zhang et al. 2016). Nevertheless, the adsorption capability remained relatively steady during the next two cycles, implying that the good regeneration ability of PEI-HOCM.

Conclusions

A novel biosorbent PEI-HOCM was prepared for removing Cr(VI) from aqueous solution. ATR-FTIR, XPS and titration analysis confirmed that the hydroxyl groups of cellulose were oxidized to carbonyl groups by H_2O_2 and PEI was successfully introduced to the HOCM. The PEI-HOCM had positively charged surface ($+20.6$ to $+86.6$ mV) at the measured pH range 3–9 according to the zeta potential analysis. The adsorption of Cr(VI) on the PEI-HOCM followed the pseudo-second-order kinetic model and the Langmuir isotherm. Its maximum adsorption capacities were 161.29, 158.73 and 147.06 mg/g at 5, 15 and 25 °C, respectively. The competitive uptakes from Na^+, Mg^{2+}, Ca^{2+}, phenol, Cl^- and NO_3^- were insignificant except SO_4^{2-} and $H_2PO_4^-$. Ionic strength had little effect on the adsorption in the range of 0–1000 mg/L NaCl. After five adsorption/desorption cycles, the adsorbent can retain good adsorption capacity. According to the obtained results from the intraparticle diffusion model, Body kinetic model and diffusion-chemisorption model, film diffusion was the rate-limiting step and chemical adsorption was the main mechanism of Cr(VI) adsorption. Meanwhile, the Cr(VI) removal involved its complete reduction into Cr(III). Hence, the prepared PEI-HOCM can be used as an effective biosorbent for Cr(VI) removal and detoxification from wastewater.

References

Alemayehu E, Thiele-Bruhn S, Lennartz B (2011) Adsorption behaviour of Cr(VI) onto macro and micro-vesicular volcanic rocks from water. Sep Purif Technol 78:55–61

Anirudhan TS, Nima J, Divya PL (2013) Adsorption of chromium(VI) from aqueous solutions by glycidylmethacrylate-grafted-densified cellulose with quaternary ammonium groups. Appl Surf Sci 279:441–449

Bal Krishna KC, Niaz MR, Sarker DC, Jansen T (2017) Phosphorous removal from aqueous solution can be enhanced through the calcination of lime sludge. J Environ Manag 200:359–365

Barrera-Diaz CE, Lugo-Lugo V, Bilyeu B (2012) A review of chemical, electrochemical and biological methods for aqueous Cr(VI) reduction. J Hazard Mater 223:1–12

Berei E, Ştefănescu O, Muntean C, Vlase T, Ţăranu BO (2018) A novel route for the preparation of $CoCr_2O_4/SiO_2$ nanocomposite starting from Co(II)–Cr(III) carboxylate complex combinations. J Mater Sci 53:4159–4172

Cai ZJ, Song XY, Zhang Q, Liu YP (2017) Amidoxime surface modification of polyindole nanofiber membrane for effective removal of Cr(VI) from aqueous solution. J Mater Sci 52:5417–5434

Cao J, Wei W, Gou GJ, Jiang M, Cui YH, Zhang SL, Wang Y, Zhou ZW (2018) Cellulose films from the aqueous DMSO/TBAH-system. Cellulose 25:1975–1986

Chen GQ, Zhang WJ, Zeng GM, Huang JH, Wang L, Shen GL (2011) Surfacemodified *Phanerochaete chrysosporium* as a biosorbent for Cr(VI) contaminated wastewater. J Hazard Mater 186:2138–2143

Chen JH, Xiang HT, Guo HX, Weng W, Hu SR, Li SX, Huang YH, Sun X, Su ZB (2014) Investigation on the adsorption properties of Cr(VI) ions on a novel graphene oxide (GO) based composite adsorbent. J Mater Chem A 2:12561–12570

Cranston ED, Gray DG, Rutland MW (2010) Direct surface force measurements of polyelectrolyte multilayer films containing nanocrystalline cellulose. Langmuir 26:17190–17197

Deng S, Ting YP (2005) Characterization of PEI-modified biomass and biosorption of Cu(II), Pb(II) and Ni(II). Water Res 39:2167–2177

Dong Z, Zhao J, Du J, Li C, Zhao L (2016) Radiation synthesis of spherical cellulose-based adsorbent for efficient adsorption and detoxification of Cr(VI). Radiat Phys Chem 126:68–74

Fierro V, Torné-Fernándezb V, Montanéb D, Celzardc A (2008) Adsorption of phenolonto activated carbons having different textural and surface properties. Microporous Mesoporous Mater 111:276–284

Gardiner ES, Sarko A (1985) Packing analysis of carbohydrates and polysaccharides. 16. The crystal structures of celluloses IV$_I$ and IV$_{II}$. Can J Chem 63:173–180

Ge YY, Li ZL (2018) Application of lignin and its derivatives in adsorption of heavy metal ions in water: a review. ACS Sustain Chem Eng 6:7181–7192

Ge H, Huang HL, Xu M, Chen Q (2016) Cellulose/poly(ethylene imine) composites as efficient and reusable adsorbents for heavy metal ions. Cellulose 23:2527–2537

Gupta VK, Ali I, Saleh TA, Siddiqui MN, Agarwal S (2013) Chromium removal from water by activated carbon developed from waste rubber tires. Environ Sci Pollut R 20:1261–1268

Hamadia NK, Chen XD, Farid MM, Lu MGQ (2001) Adsorption kinetics for the removal of chromium(VI) from aqueous solution by adsorbents derived from used tyres and sawdust. Chem Eng J 84:95–105

Ho YS (2004) Selection of optimum sorption isotherm. Carbon 42:2115–2116

Hu J, Lo IMC, Chen G (2005) Fast removal and recovery of Cr(VI) using surface-modified jacobsite (MnFe$_2$O$_4$) nanoparticles. Langmuir 21:11173–11179

Jiang YL, Liu ZF, Zeng GM, Liu YJ, Shao BB, Li ZG, Liu Y, Zhang W, He QY (2018) Polyaniline-based adsorbents for removal of hexavalent chromiumfrom aqueous solution: a mini review. Environ Sci Pollut Res 25:6158–6174

Karthikeyan T, Rajgopal S, Miranda LR (2005) Chromium(VI) adsorption from aqueous solution by *Hevea brasiliensis* sawdust activated carbon. J Hazard Mater 124:192–199

Kaya M, Odabasi M, Mujtaba M, Sen M, Bulut E, Akyuz B (2016) Novel three-dimensional cellulose produced from trunk of *Astragalus gummifer* (Fabaceae) tested for protein adsorption performance. Mater Sci Eng C 62:144–151

Kera NH, Bhaumik M, Ballav N, Pillay K, Ray SS, Maity A (2016) Selective removal of Cr(VI) from aqueous solution by polypyrrole/2,5-diaminobenzene sulfonic acid composite. J Colloid Interface Sci 476:144–157

Ko YG, Choi US, Kim TY, Ahn DJ, Chun YJ (2002) FT-IR and isotherm study on anion adsorption onto novel chelating fibers. Macromol Rapid Commun 23:535–539

Kumar ASK, Jiang SJ, Tseng WL (2015) Effective adsorption of chromium(VI)/Cr(III) from aqueous solution using ionic liquid functionalized multiwalled carbon nanotubes as a super sorbent. J Mater Chem A 3:7044–7057

Kumari S, Mankotia D, Chauhan GS (2016) Crosslinked cellulose dialdehyde for Congo red removal from its aqueous solutions. J Environ Chem Eng 4:1126–1136

Leila N, Asghar L, Hakimeh S (2018) Chestnut oak shells activated carbon: preparation, characterization and application for Cr(VI) removal from dilute aqueous solutions. J Clean Prod 185:554–561

Li HL, Wu B, Mu CD, Lin W (2011) Concomitant degradation in periodate oxidation of carboxymethyl cellulose. Carbohydr Polym 84:881–886

Lin FC, You YZ, Yang X, Jiang X, Liu QL (2017) Microwave-assisted facile synthesis of TEMPO-oxidized cellulose beads with high adsorption capacity for organic dyes. Cellulose 24:5025–5040

Liu J, Yan M, Zhang YK, Du KF (2011) Study of glutamate-modified cellulose beads for Cr(III) adsorption by response surface methodology. Ind Eng Chem Res 50:10784–10791

Ma Y, Liu WJ, Zhang N, Li YS, Jiang H, Sheng GP (2014) Polyethylenimine modified biochar adsorbent for hexavalent chromium removal from the aqueous solution. Bioresour Technol 169:403–408

Miretzky P, Cirelli AF (2010) Cr(VI) and Cr(III) removal from aqueous solution by raw and modified lignocellulosic materials: a review. J Hazard Mater 180:1–19

Qi HS, Cai J, Zhang LN, Kuga S (2009) Properties of films composed of cellulose nanowhiskers and a cellulose matrix regenerated from alkali/urea solution. Biomacromolecules 10:1597–1602

Qian H, Lin YL, Xu B, Wang LP, Cao ZC, Cao NY (2018) Adsorption of haloforms onto GACs: effects of adsorbent properties and adsorption mechanisms. Chem Eng J 349:849–859

Qiu B, Guo J, Zhang X, Sun DZ, Gu HB, Wang Q, Wang HW, Wang XF, Zhang X, Weeks BL, Guo ZH, Wei SY (2014) Polyethylenimine facilitated ethyl cellulose for hexavalent chromium removal with a wide pH range. ACS Appl Mater Interfaces 6:19816–19824

Safari M, Khataee A, Darvishi CSR, Rezaee R (2018) Ultrasonically facilitated adsorption of an azo dye onto nanostructures obtained from cellulosic wastes of broom and cooler straw. J Colloid Interface Sci 522:228–241

Sathvika T, Manasi Rajesh V, Rajesh N (2015) Microwave assisted immobilization of yeast in cellulose biopolymer as a green adsorbent for the sequestration of chromium. Chem Eng J 279:38–46

Setyono D, Valiyaveettil S (2016) Functionalized paper-A readily accessible adsorbent for removal of dissolved heavy metal salts and nanoparticles from water. J Hazard Mater 302:120–128

Stypula B, Stoch J (1994) The characterization of passive films on chromium electrodes by XPS. Corros Sci 36:2159–2167

Sudur F, Orbey N (2015) Properties of hydrogen peroxide encapsulated in silica hydrogels and xerogels. Ind Eng Chem Res 54:11251–11257

Sun Q, Yang L (2003) The adsorption of basic dyes from aqueous solution on modified peat–resin particle. Water Res 37:1535–1544

Sun XT, Yang LR, Xing HF, Zhao JM, Li XP, Huang YB, Liu HZ (2013) Synthesis of polyethylenimine-functionalized poly(glycidyl methacrylate) magnetic microspheres and their excellent Cr(VI) ion removal properties. Chem Eng J 234:338–345

Sun XT, Yang LR, Li Q, Zhao JM, Li XP, Wang XQ, Liu HZ (2014) Amino-functionalized magnetic cellulose nanocomposite as adsorbent for removal of Cr(VI): synthesis and adsorption studies. Chem Eng J 241:175–183

Tan IAW, Chan JC, Hameed BH, Lim LLP (2016) Adsorption behavior of cadmium ions onto phosphoric acid-impregnated microwave-induced mesoporous activated carbon. J Water Process Eng 14:60–70

To MH, Hadi P, Hui CW, Lin CSK, McKay G (2017) Mechanistic study of atenolol, acebutolol and carbamazepine adsorption on waste biomass derived activated carbon. J Mol Liq 241:386–398

Tokuyama H, Ishihara N (2010) Temperature-swing adsorption of precious metal ionsonto poly(2-(dimethylamino)ethyl methacrylate) gel. React Funct Polym 70:610–615

Velempini T, Pillay K, Mbianda XY, Arotiba OA (2017) Epichlorohydrin crosslinked carboxymethyl cellulose-ethylenediamine imprinted polymer for the selective uptake of Cr(VI). Int J Biol Macromol 101:837–844

Wang SL, Lee JF (2011) Reaction mechanism of hexavalent chromium with cellulose. Chem Eng J 174:289–295

Wang S, Li H, Xu L (2006) Application of zeolite MCM-22 for basic dye removal from wastewater. J Colloid Interface Sci 295:71–78

Wang W, Bai Q, Liang T, Bai HY, Liu XY (2017) Two-sided surface oxidized cellulose membranes modified with PEI: preparation, characterization and application for dyes removal. Polymers 9:455–468

Yan YZ, An QD, Xiao ZY, Zheng W, Zhai SR (2017) Flexible core-shell/bead-like alginate@PEI with exceptional adsorption capacity, recycling performance toward batch and column sorption of Cr(VI). Chem Eng J 313:475–486

Zhang SD, Zhang YR, Wang XL, Wang YZ (2009) High carbonyl content oxidized starch prepared by hydrogen peroxide and its thermoplastic application. Starch-Starke 61:646–655

Zhang YW, Xu L, Zhao L, Peng J, Li CC, Li JQ, Zhai ML (2012) Radiation synthesis and Cr(VI) removal of cellulose microsphere adsorbent. Carbohydr Polym 88:931–938

Zhang N, Zang GL, Shi C, Yu HQ, Sheng GP (2016) A novel adsorbent TEMPO-mediated oxidized cellulose nanofibrils modified with PEI: preparation, characterization, and application for Cu(II) removal. J Hazard Mater 316:11–18

Zhang CZ, Su JJ, Zhu HX, Xiong JH, Liu XL, Li DX, Chen YM, Li YH (2017a) The removal of heavy metal ions from aqueous solutions by amine functionalized cellulose pretreated with microwave-H_2O_2. RSC Adv 7:34182–34191

Zhang LM, Ge HH, Xu M, Cao J, Dai YJ (2017b) Physicochemical properties, antioxidant and antibacterial activities of dialdehyde microcrystalline cellulose. Cellulose 24:2287–2298

Zhang SL, Wang ZK, Chen HY, Kai CC, Jiang M, Wang Q, Zhou ZW (2018) Polyethylenimine functionalized Fe_3O_4/steam-exploded rice straw composite as an efficient adsorbent for Cr(VI) removal. Appl Surf Sci 440:1277–1285

Zhao FP, Repo E, Song Y, Yin DL, Hammouda SB (2017) Polyethylenimine-cross-linked cellulose nanocrystals for highly efficient recovery of rare earth elements from water and a mechanism study. Green Chem 19:4816–4828

Zheng CF, Zheng HL, Wang YJ, Wang YL, Qu WQ, An Q, Liu YZ (2018) Synthesis of novel modified magnetic chitosan particles and their adsorption performance toward Cr(VI). Bioresour Technol 267:1–8

Zhou Y, Jin Q, Zhu T, Akama Y (2011) Adsorption of chromium(VI) from aqueous solutions by cellulose modified with beta-CD and quaternary ammonium groups. J Hazard Mater 187:303–310

Zhou Q, Yan CJ, Luo WJ (2016) Polypyrrole coated secondary fly ash-iron composites: novel floatable magnetic adsorbents for the removal of chromium(VI) from wastewater. Mater Des 92:701–709